Tikrit Journal of Engineering Sciences (2022) 29 (3): 70-81
DOI: http://doi.org/10.25130/tjes.29.3.8

IRAQI Academic Scientific Journals

ISSN: 1813-162X (Print); 2312-7589 (Online)

Tikrit Journal of Engineering Sciences

available online at: http://www.tj-es.com

TJES Tikrit Journal of Engineering Sciences

Power Sharing and Frequency Control in Inverter-based Microgrids

Sazgar Abdualaziz Wali [*] , **Aree Akram Muhammed**

Electrical Department, College of Engineering, Salahaddin University, Erbil, Iraq.

Keywords:

Microgrid; Power Sharing; Frequency Control; MPPT; PID controller; PLL

ARTICLE INFO

Article history:

Received	19 Dec. 2021
Accepted	20 Feb. 2022
Available online	15 Nov. 2021

Citation: Wali SA, Muhammed AA. Power Sharing and Frequency Control in Inverter-based Microgrids. Tikrit Journal of Engineering Sciences 2022; 29(3): 70- 81. **http://doi.org/10.25130/tjes.29.3.8**

ABSTRACT

In the recent period, developed countries have resorted to using smart grids more widely as a solution to the problems of shortage of electric power, because it is the most environmentally friendly due to its reliance on renewable energy sources and does not require expensive maintenance due to the proximity of its stations to the feeding areas. However, these networks faced problems in sharing the required power between the inverters of the user stations, as well as regulating their frequency when connected to the main network to fill the shortage of electrical energy. This paper aims to achieve the actual sharing of power (Active and Reactive) supply to the varying load between the smart grid inverters by designing a PID (Proportional, Integral, Derivative) controller. PID controller gain tuning by PSO (particle swarm optimization) algorithm which is based on PWM (Pulse Width Modulation) scaler that feeds the Microgrid inverter switches. Frequency control can be achieved when connecting Microgrid with the main grid by using PLL (Phase Locked Loop) to generate a controlled reference signal for the PID controller.

[*] Corresponding author: E-mail: eng.sazi89@gmail.com, Electrical Department, College of Engineering, Salahaddin University, Erbil, Iraq.

تقاسم الطاقة والتحكم في التردد في الشبكات المصغرة القائمة على العاكس

سازكار عبد العزيز ولي قسم الهندسة الكهربائية / كلية الهندسة / جامعة صلاح الدين / أربيل - العراق.
اري أكرم محمد قسم الهندسة الكهربائية / كلية الهندسة / جامعة صلاح الدين / أربيل - العراق.

الخلاصة

في الآونة الاخيرة لجأت الدول المتقدمة الى استخدام الشبكات الذكية على نطاق اوسع باعتبارها حل لمشاكل نقص الطاقة، ولعدة اسباب اخرى كونها صديقة للبيئة بسبب اعتمادها على مصادر الطاقة المتجددة، لا تتطلب تكلفة باهظة وسهولة صيانتها لقرب محطاتها من مناطق التغذية. ومع ذلك, فان هذه الشبكات واجهت مشاكل في تقاسم الطاقة المطلوبة بين محولات المحطات المستعملة كذلك مشكلة اختلاف التردد عند العمل بوضع الاتصال بالشبكة الرئيسية في اوقات الذروة .الهدف من البحث هو تحقيق المشاركة الفعلية بين المحطات المغذية للأحمال الكهربائية المتغيرة ,وذلك من خلال تصميم وحدة تحكم(متناسبة-متكاملة-مشتقة) وضبطها عن طريق استعمال طرق التحسين المعتمدة على اساس السرب واستعمال عاكس تعتمد على تقنية تعديل عرض النبض ز ويتم تحقيق التحكم بالتردد عند الاتصال بالشبكة لسد النقص في التجهيز للطاقة باستعمال محكم حلقة غلق الطور.

الكلمات الدالة: التحكم في التردد، تحكم PID ، تقاسم الطاقة.

1. INTRODUCTION

Due to the energy crisis and the highly prominent environmental issues, the human community has gathered to develop power plants based on renewable energy sources with low carbon and build a high environmental civilization that helps human and economic sustainability. Countries of the world such as the United States, European countries, and Japan have resorted to conducting numerous research on the small grid system and put forward the concept of smart grids in terms of distributed energy, load, energy storage devices, and control devices. formed many power systems that supply energy in a controlled and highly reliable manner by relying on local energies [1]. For example, North America generates an operating capacity of about 2,088 MW according to [2]and Europe comes in second place, with an operating capacity of about 384 MW, It is followed by the Asia Pacific region, with a capacity of 303MW, and the capacity of microgrids in the rest of the world is about 404MW. The microgrid is defined as a group of distributed energy sources (DESs), including renewable energy sources (RESs) and energy storage systems (ESS), released to the loads connected to them, which work as a unified system that can be controlled. Microgrids exist in different sizes, they may be complex and large networks that may reach tens of megawatts (MW), or they may be small systems within the range of hundreds of kilowatts (kW) where they supply a small number of customers. The microgrid has many configurations depending on its size and function, it may be located connected to the main network in grid-connecting mode (GCM) or isolated from it in island mode (IM). In (GCM) which is used to fill the shortage in feeding the load, the microgrid must contain a point of interconnection (POI) or the so-called point of common coupling (PCC) with the large main grid. The smart grid should have the possibility of a smooth transition to an island mode that does not require both (PIO) and (PCC) [3]. Microgrids face problems in addition to their high advantages, including the production of electrical energy, which varies according to renewable energy sources, for example, solar energy generation depends on the efficiency of solar cells, the intensity of radiation, and the temperature of the sun at that time. This raises concerns about the quality of the generated energy because it depends on characteristics related to the irregular fluctuation in energy sources [4]. This problem is addressed by increasing battery energy storage systems or adopting a hybrid system from several energy sources such as adding wind turbines or diesel generators to reduce volatility due to climatic conditions [5]. Microgrids consist of several main parts including the renewable energy source (RESs) which generate electrical energy such as solar energy by using a PV (photovoltaic) array. This energy is amplified to the required level by passing it through converters that have several different types, the most common of which is DC to DC boost converter, the required energy coming out of the converter, which is in the form of continuous energy, is often converted into alternating energy by using the third part of the microgrid, which is the inverter that passes the AC output from the inverter through the filter to obtain a pure sine wave that supplies the load connected to it, as shown in Fig .1 [6].

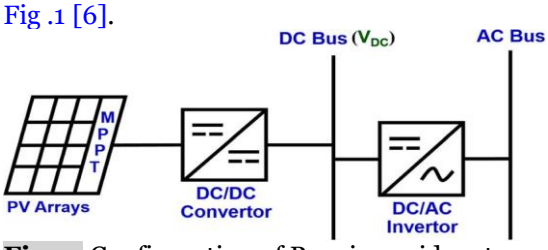

Fig .1. Configuration of Pv microgrid system.

2.DC/DC BOOST CONVERTER WITH MPPT ALGORITHM.

This type of converter is connected to one of the types of renewable energy sources, for example, the Photovoltaic (PV) Array, according to projections by the International Energy Agency (IEA), photovoltaic energy represents about half of the development of renewable energy generation systems. Governments and market policies encourage the use of photovoltaic energy in renewable energy systems due to its many advantages, including its low cost and accurate modeling, and it is considered the most pioneering energy than other types of renewable energies. The value of the photons that generate current changes with the change in temperature and radiation. Over the years, scientists have tried to reduce losses that occur by using photovoltaic energy and making solar panels work at an optimal operating point in various weather conditions. One of the most problems facing photovoltaic panels is the problem of partial shading condition (PSC). The serial connection of the panels is more susceptible to the problem of (PSC), but the panels connected in parallel are more flexible with the problem of partial shading problem. Partial shading losses are reduced by following steps [7]: (1) the integration of the bypass diodes. (2) the application of tracking techniques for global peak energy. (3) the use of PV arrays according to the prominent pattern distortion. (4) reconfiguring the PV arrays to obtain the maximum power. This type of converter is widely used with non-uniform DC sources obtained from PV arrays that change in efficiency with the change in the amount of radiation and heat absorbed by the sun over time. The converter circuit consists of four main parts, an electronic switch inductor, a diode, and an output capacitor as shown in Fig .2 [8].

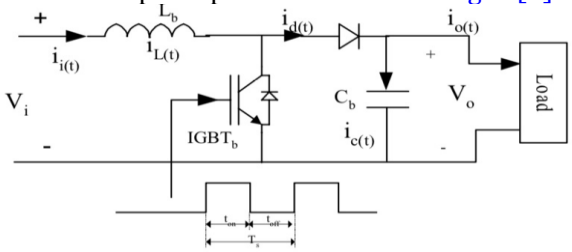

Fig .2. DC/DC Boost Converter Circuit.

The DC/DC boost converter is designed from two main parameters, the inductor and the capacitor, which are calculated by calculating the duty cycle for the input and output voltages as shown in equation (1) [9].

$$D = 1 - \frac{V_{in}}{V_{out}} \quad \text{... (1)}$$

Where v_{in} is the input voltage, v_{out} is the output voltage, D is the duty cycle ratio, and The converter inductor and capacitor are each calculated from the equations(2), and (3) below [9].

$$L = \frac{D*(1-D)^2*RL}{2*F_S} \quad \text{... (2)}$$

$$C = \frac{D}{RL*r*F_S} \quad \text{..... (3)}$$

L is an inductor, RL is a resistive load, F_s is switching frequency, C is the output capacitor and (r) is the ripple factor equal to 1% [10]. Depending on the storage capacity of the converter and the relative length of the period of connecting the electronic switch, the converter operates in two modes, the first is the continuous connection mode (CCM) when the IGBT transistor is on, and the second mode is the dis-continuous connection mode(DCM) when the switch is off [8]. To control the average DC voltage output, the amount of power absorbed from the source must be regulated by means of a maximum power point tracking controller (MPPT). Each PV (photovoltaic) array has its pv curve specification which is the maximum power that the source can give without damaging it or disrupting it. There are several ways to write the MPPT algorithm Including the (Perturb and Observe) P&O method used in the research [11].

3.DC/AC INVERTER BASED ON PWM SCALER AND PID CONTROLLER

Three phase inverter with a topology of four legs based on a PWM(Pulse Width Modulation) scaler and PID controller to control the reference signal of PWM fits all (balanced, unbalanced, and nonlinear) load cases [12] as shown in Fig.3 used to convert DC voltage or current to sine wave with many harmonics. Inverters can be divided into three types according to the way the inverter is equipped with energy, which are: **(1)** Current source inverter (CSI). **(2)** Impedance source inverter (z-source inverter or ZSI). **(3)** Voltage source inverter (VSI). Inverters use the configuration of DC/AC converters. Inverters are divided according to the formation of their circuit as well into five types, namely: Three-phase full-bridge current source inverter (CSI), Soft switching inverter, Single-phase half-bridge voltage source inverter (VSI), Single-phase full-bridge (VSI), and Three-phase full-bridge (VSI) [13]. Three-phase inverters with a topology of four legs designed from 4-leg are connected, three of which are 3 phase, and the fourth leg represents the neutral, the topology of the inverter consists of eight electronic switch, which is an IGBT transistor that depends on thePWM method to open and close it. The switches called SA, SB, SC and SN are called upper switches, which produce the positive portion of the sine wave, and the SA', SB', SC' and SN' switches are called lower switches that are open to displaying the negative portion of the sine wave.

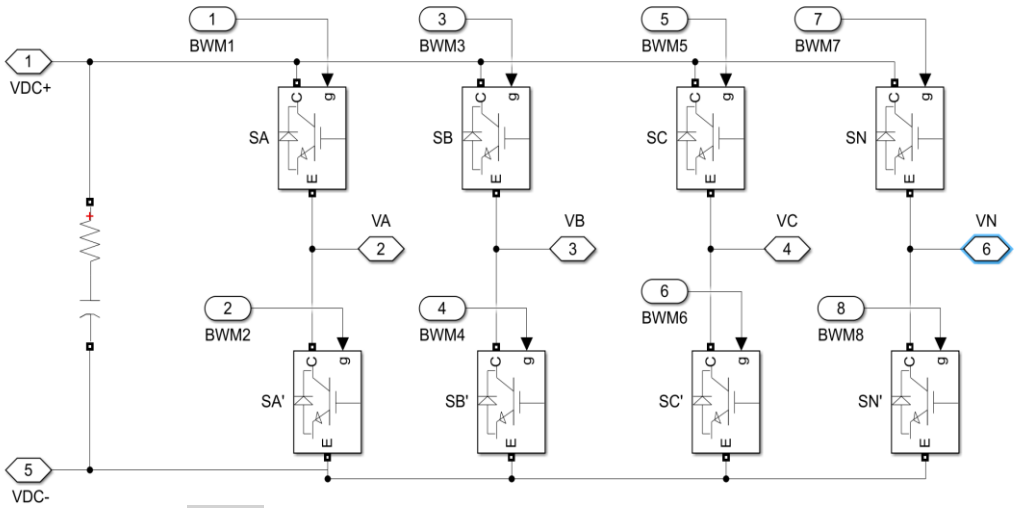

Fig.3. Three-Phase Inverter with Four Leg Topology.

Pulse width modulation (PWM) is a powerful technique for controlling analog circuits using digital outputs because the analog signal has a value that varies with time, and to control the change in electronic devices, PWM technology is used [14]. The PWM technology converts the sinusoidal signal into digital with the same amplitude, but with different dimensions, which allows changing the amount of time in which the signal is at a high value, the so-called duty cycle or on time. The duty cycle expresses in percentage, which is equal to the reciprocal of the frequency of the reference signal. If the signal value is high for half the time and low for half the time, the duty cycle may be equal to about 50%, the waveform is square, and the ratio can be less or more in one signal. This technique is practically done by comparing (modeling) the sine wave signal as a reference signal with the frequency required for the inverter outputs (fundamental frequency) with the carrier signal with a high frequency equal to tens of times the fundamental frequency for the inverter outputs. After converting the analog signal into a digital signal of a certain frequency, it connects the electronic switch gates of the inverter as shown in Fig.3 to convert both the current and DC voltage to AC [13]. The LC filter is used to get rid of the harmonics present in the output voltage wave of the inverter, which causes large power losses in the form of high heat in the loads and leads to damage to the loads connected to the grid. The LC filter is designed from two parameters, the inductor, and the capacitor, according to the type of inverter designed, and they are calculated from the two equations(4), and (5) below [15].

$$L_{max} = \frac{3*V_n^2}{10*\omega_O*S_n} \quad \ldots (4)$$

$$C_F = \frac{0.05*P_n}{3*\omega_O*V_n^2} \quad \ldots (5)$$

Where V_n is voltage line to line, ωo is the fundamental frequency,S_n Is appearance power and P_n is rated power. The PID controller is used as a kind of closed-loop controller, as it relies on one of the system's parameters, which brings it a value or a signal, and on its basis, it organizes the work of the system as shown in Fig.4. From its name, it combines proportional, integrated, and derived control units. The purpose of using PID is to force the system to work according to a specific point or wave. It is preferable to use a PID controller due to its small mass, the speed of its interaction with the changes taking place in the system, and its high efficiency in bringing the system back to the desired point and level. Fig.5 shows the step response of the system (rise time, settling time, overshoot, and steady-state error) that affect the gain values for a proportional controller (K_P), integral controller (K_i) and derivative controller (K_d) of the PID controller [16].

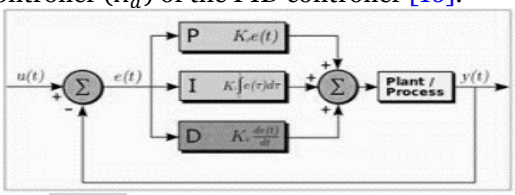

Fig.4. Closed Loop PID Controller.

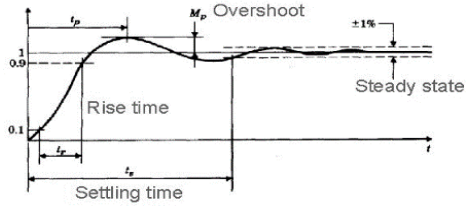

Fig.5. Step Response of the System.

The selected controller gains affect the step response of the system, each one differently. For example, the (K_P) reduces the rise time, affects a little in the settling time, increases overshoot with its increase, and in turn reduces

the steady state error time. As for the (K_i), it slightly changes the rise time, reduces the settling time, reduces the over-shoot, and does not affect the steady-state error time, and for the (K_d), it is reducing rise time, increases by the settling time, increases the over-shoot, and it eliminates steady state error time [17]. The behavior of three-phase systems is given by the equation of voltage and current and its change with time, so the mathematical modeling for these systems is very difficult and must be converted to two-phase using the Park and Clark Transformation Method to convert to DQo frame as shown in the equations below [12].

$$E_{AN} = (SA - SN)\ Vdc \ldots\ldots \textbf{(6)}$$
$$E_{BN} = (SB - SN)\ Vdc \ldots\ldots \textbf{(7)}$$
$$E_{CN} = (SC - SN)\ Vdc \ldots\ldots \textbf{(8)}$$

Where E_{AN}, E_{BN} and E_{CN} are output voltage, SA, SB, SC, and SN are control signals for four leg inverter, if equal to 1 that means the upper switches close and open lower switches else equal to 0 the upper switches open and lower close. Vdc is the input DC voltage of the inverter. The mathematical model in ABC coordinates for the system can be written as equations (9), and (10) below.

$$\begin{bmatrix} E_{AN} \\ E_{BN} \\ E_{CN} \end{bmatrix} = L\frac{d}{dt}\begin{bmatrix} I_A \\ I_B \\ I_C \end{bmatrix} + \begin{bmatrix} V_A \\ V_B \\ V_C \end{bmatrix} \ldots \textbf{(9)}$$

$$\begin{bmatrix} I_A \\ I_B \\ I_C \end{bmatrix} = \begin{bmatrix} I_{LA} \\ I_{LB} \\ I_{LC} \end{bmatrix} + C\frac{d}{dt}\begin{bmatrix} V_A \\ V_B \\ V_C \end{bmatrix} \ldots \textbf{(10)}$$

Where I_{LA}, I_{LB} and I_{LC} are currents after the filter. The matrix that transforms the ABC system into the QDo system is represented by equation (11) below.

$$T = \frac{2}{3}\begin{bmatrix} cos(\omega t) & cos\left(\omega t - \frac{2\pi}{3}\right) & cos\left(\omega t + \frac{2\pi}{3}\right) \\ -\sin(\omega t) & -sin(\omega t - \frac{2\pi}{3}) & -sin(\omega t + \frac{2\pi}{3}) \\ \frac{1}{2} & \frac{1}{2} & \frac{1}{2} \end{bmatrix} \ldots \textbf{(11)}$$

Where ω is the angular frequency of the current, the voltage and the current in QDo can be represented as the equation (12), (13):

$$\begin{bmatrix} E_D \\ E_Q \\ E_0 \end{bmatrix} = T\begin{bmatrix} E_{AN} \\ E_{BN} \\ E_{CN} \end{bmatrix} \ldots \textbf{(12)}$$

$$\begin{bmatrix} I_D \\ I_Q \\ I_0 \end{bmatrix} = T\begin{bmatrix} I_A \\ I_B \\ I_C \end{bmatrix} \ldots \textbf{(13)}$$

By substituting equation No. (12) and (13) in Equations No. (9) and (10), it becomes as follows:

$$\begin{bmatrix} E_D \\ E_Q \\ E_0 \end{bmatrix} = L\frac{d}{dt}\begin{bmatrix} I_D \\ I_Q \\ I_0 \end{bmatrix} + \omega L\begin{bmatrix} -I_Q \\ I_D \\ 0 \end{bmatrix} + \begin{bmatrix} V_D \\ V_Q \\ V_0 \end{bmatrix} \ldots \textbf{(14)}$$

$$\begin{bmatrix} I_D \\ I_Q \\ I_0 \end{bmatrix} = \begin{bmatrix} I_{LD} \\ I_{LQ} \\ I_{L0} \end{bmatrix} + C\frac{d}{dt}\begin{bmatrix} V_D \\ V_Q \\ V_0 \end{bmatrix} + \omega C\begin{bmatrix} -V_Q \\ V_D \\ 0 \end{bmatrix} \ldots \textbf{(15)}$$

Where (V_D,V_Q,V_0),(I_{LD},I_{LQ},I_{L0})are the voltage and current of the load respectively. From equation (14) the voltage droop on LC filter inductance can be written as equation (16):

$$\begin{bmatrix} V_{FD} \\ V_{FQ} \\ V_{F0} \end{bmatrix} = L\frac{d}{dt}\begin{bmatrix} I_D \\ I_Q \\ I_0 \end{bmatrix} \ldots \textbf{(16)}$$

The amount of the PID controller gains used to control the system in QDo coordinate.PID controller provides references to voltage drop by current feedback control.

$$\begin{bmatrix} V_{FD} \\ V_{FQ} \\ V_{F0} \end{bmatrix} = (K_P + K_i/s + K_d\, s)\begin{bmatrix} I_{D'} - I_D \\ I_{Q'} - I_Q \\ I_{0'} - I_0 \end{bmatrix} \ldots \textbf{(17)}$$

And by substituting equation No. (17) into Equation No. (14), it becomes as follows:

$$\begin{bmatrix} E_D \\ E_Q \\ E_0 \end{bmatrix} = (K_P + K_i/s + K_d\, s)\begin{bmatrix} I_{D'} - I_D \\ I_{Q'} - I_Q \\ I_{0'} - I_0 \end{bmatrix} + \omega L\begin{bmatrix} -I_Q \\ I_D \\ 0 \end{bmatrix} + \begin{bmatrix} V_D \\ V_Q \\ V_0 \end{bmatrix} \ldots \textbf{(18)}$$

Where $I_{D'}$, $I_{Q'}$, $I_{0'}$ are references value of output current of inverse when PID interacts with a capacitor of the LC filter, which becomes:

$$C\frac{d}{dt}\begin{bmatrix} V_D \\ V_Q \\ V_0 \end{bmatrix} = (K_P + K_i/s + K_d\, s)\begin{bmatrix} V_{D'} - V_D \\ V_{Q'} - V_Q \\ V_{0'} - V_0 \end{bmatrix} \ldots \textbf{(19)}$$

Where $V_{D'}$, $V_{Q'}$,$V_{0'}$ are references value of load voltage by substituting equation No. (19) into Equation No. (15), it becomes as follows:

$$\begin{bmatrix} ID \\ IQ \\ I0 \end{bmatrix} = \begin{bmatrix} ILD \\ ILQ \\ IL0 \end{bmatrix} + (K_P + K_i/s + K_d s)\begin{bmatrix} V_{D'} - V_D \\ V_{Q'} - V_Q \\ V_{0'} - V_0 \end{bmatrix} + \omega C\begin{bmatrix} -VQ \\ VD \\ 0 \end{bmatrix} \ldots \textbf{(20)}$$

4.TRANSFER FUNCTION OF THE SYSTEM AND TUNNING OF PID CONTROLLER BY PSO TECHNIQUE.

The transfer function is defined as the ratio of the Laplace transform of output to the Laplace transform of input when all initial conditions are zero. To find the transfer function of the microgrid designed as in Fig.6 consisting of an LC filter connected to any type of load represented by the symbol RL.

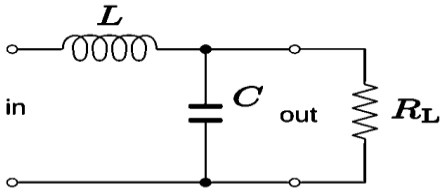

Fig .6. LC-Filter with Connected Load.

To convert the LC filter circuit connected to the RL load to the S-domain, the inductor becomes SL and the capacitor 1/SC, and the RL load remains as it is, assuming that it is a resistive load. The circuit is shortened by adding the parallel sides together, i.e. 1/SC // RL as shown below.

$$ZC = \frac{RL*(\frac{1}{SC})}{RL+(\frac{1}{SC})} = \frac{RL}{1+SC\ RL} \ldots \textbf{(21)}$$

$$Transfer\ Function = \frac{V_{out}}{V_{in}} = G(s) = \frac{ZC}{ZC+SL} \ldots \textbf{(22)}$$

And by substituting equation (21) into equation (22), the transfer function of Fig.6 is represented by equation (23) below.

$$G(s) = \frac{(\frac{1}{LC})}{S^2+S(\frac{1}{(C*RL)})+1/(LC)} \quad \text{... (23)}$$

The gains of the PID controller (K_P, K_i, K_d) are determined by a practical swarm optimization (PSO) technique that depends on the transfer function of the microgrid shown in equation (23), The PSO algorithm depends on the social behavior of animals such as insects, birds, and fish. In particular, the cooperative method adopted by the members of one swarm to find food, where each member of the swarm changes the search pattern according to his own experiences. This technique is characterized by simultaneously searching in a large area to find the area in which the optimal solution lies [18]. All these things must be specified: the objective function (the function it is desired maximum or minimum), the decision variable (a quantity that the decision-maker controls), and the search space to be able to write a PSO algorithm. PSO follows this procedure in its performance first initializations by giving initial values of the population (N), initial values of position (X), and velocity (V). Second, update both the position and velocity through the two equations (10 & 11) below. Thirdly and finally, the counter is increased by one until you operate according to the required number of attrition [19].

$$V_i(t) = w * V_i\,(t-1) + c_1 * r_1\big(P_{best\,i} - X_i(t-1)\big) + c_2 * r_2\big(g_{best} - X_i(t-1)\big) \text{ ... (24)}$$

$$X_i(t) = X_i(t-1) + V_i(t) \quad \text{... (25)}$$

Where

$V_i(t)$ is the velocity for a new iteration.

$V_i\,(t-1)$ is the velocity for the previous iteration.

$X_i(t)$ is the position for a new iteration.

$X_i(t-1)$ is the position for the previous iteration.

w is inertia weight.

c_1 *and* c_2 are individual and social cognitive.

r_1 and r_2 are a random number in the range (0-1).

5.CONNECTING MODE OF MICROGRID WITH PHASE-LOCKED LOOP (PLL)

There are two modes in which the microgrid operates, island mode, is called when the smart grid supplies the loads alone and without connecting them to the main grid. In peak times and insufficient power is supplied by the microgrid, the main grid is used to fill the shortage, in this case, the microgrid work in a grid-connecting mode. When connecting the two grids with the same load, the loads will face the problem of incompatibility in the frequency of the voltage and the current waves supplied by two different grids, so it needs a controller that regulates the frequency. In the design, phase-locked loop(PLL) control was used, which regulates the phase of the two waves. Phase locked loop (PLL) is a control unit that generates an output signal whose phase is related to the phase of the input signal. PLL has several types, but the simplest of them consists of an electronic circuit, as shown in Fig .7, which consists of a detector, that compares the input phase with the phase of the feedback signal. filter loop, a filter may be a low pass filter, which passes frequencies lower than the cut-off frequency and prevents the passage of frequencies higher than the frequencies above the cut-off. variable frequency oscillator whose frequency is determined by the applied voltage, which is why it is called a voltage-controller oscillator [20].

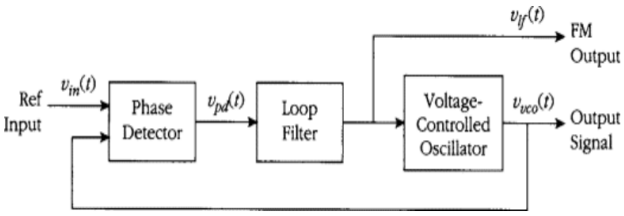

Fig .7. Phase Locked Loop Block Diagram

The oscillator generates a periodic signal at a specific frequency and with feedback, it is compared through the detector with the periodic signal of the input thus the phase is adjusted, and maintaining the input and output phase means maintaining the frequency of both. The PLL controller is used in the microgrid if it is connected to the main network in the grid- connecting mode clauses work to control the phase of the two networks feeding the same load without any difference in their frequencies.

6.DESIGNED CIRCUIT AND SIMULATION RESULT

The mathematical equations and circuits designed using the MATLAB/ SIMULINK program with Simescap tools are applied to receive the results after determining the parameters of the system as shown in Table 1 below. The designed smart grid circuit can be illustrated in Fig.8.

Table 1. Main parameter of the system

parameters	values
Inverter DC voltage input	Vdc= 800 v
Sampling time	T_s = 2µS
Switching frequency	F_s = 5000 Hz
Fundamental frequency	F= 50 Hz
DC capacitance link	C_{dc} = 1000µF
LC filter	L_{max}= 1.5mH , C_F= 100µF

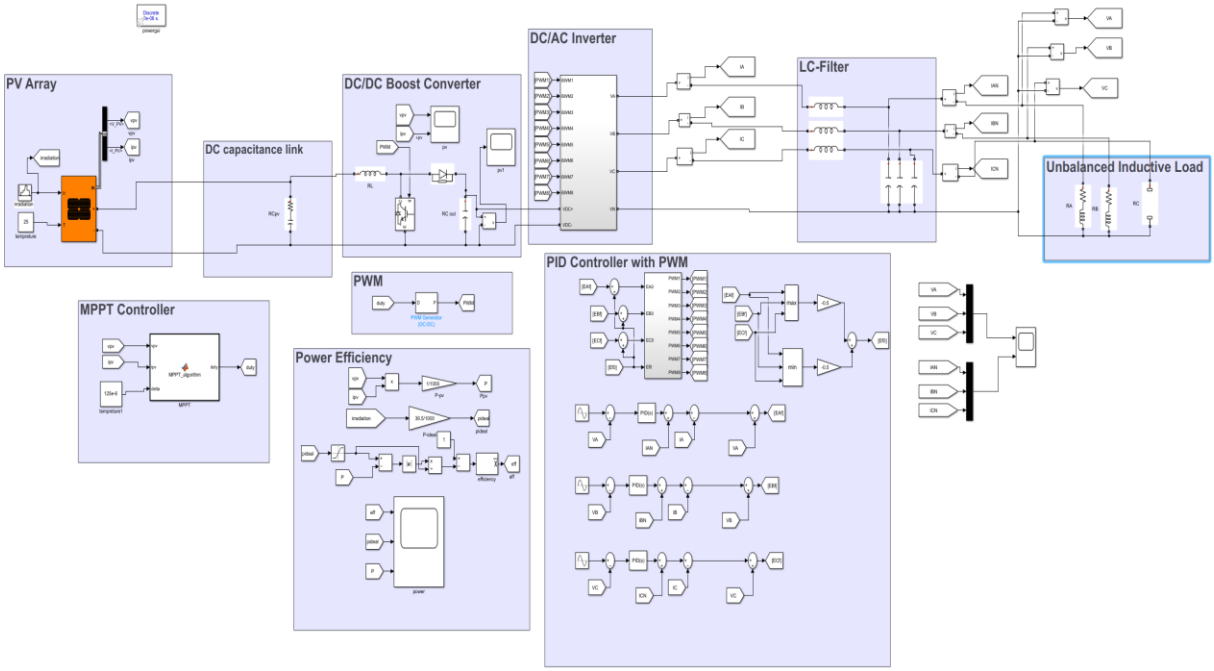

Fig.8. Designed PV Micro Grid Connected to Linear Unbalanced Inductive Loads simulated by Matlab.

The circuit in Fig.8 consists of a pv generator with a boost converter to amplify the dc voltage to the required amount and thus pass it through a 4-leg inverter topology as in Fig .9 to convert the DC voltage to AC and then depend on the LC filter to obtain a pure sine wave voltage and current free of harmonics to feed different types of loads connected to the circuit as shown in Table 2.

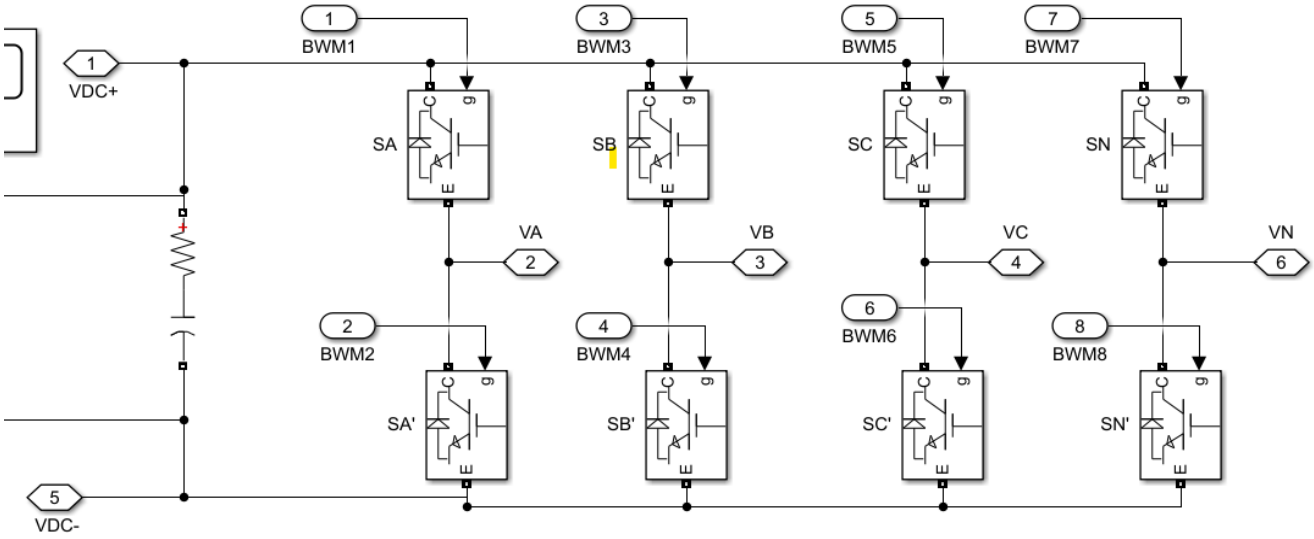

Fig.9. Three Phase 4-leg Inverter Topology.

Table 2. Different load parameter

Case	Load parameter value
1- Balanced resistive load	(RA, RB, RC) = 15Ω
2- Unbalanced resistive load	RA= 5 Ω, RB=10 Ω, RC=∞
3- Balanced inductive load	(RA, RB, RC) = 10Ω (LA, LB, LC) = 20 mH
4-Unbalanced inductive load	RA= 5 Ω, RB=10 Ω, RC=∞ LA= 10mH ,LB= 30 mH
5-Nonlinear unbalanced load	RA= 20 Ω, LA= 50 mH RB1= 1 Ω, RB2=60 Ω, CB=3000 µF RC=70 Ω, LC=20 mH,Cc=5000 µF

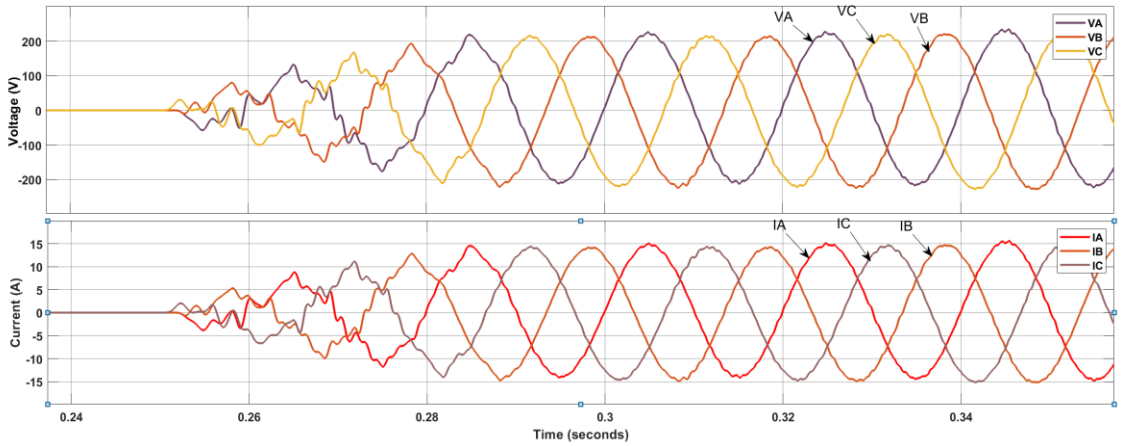

Fig. 10. Three Phase Voltage and Current for Micro Grid Connected to Linear Balanced Resistive Loads.

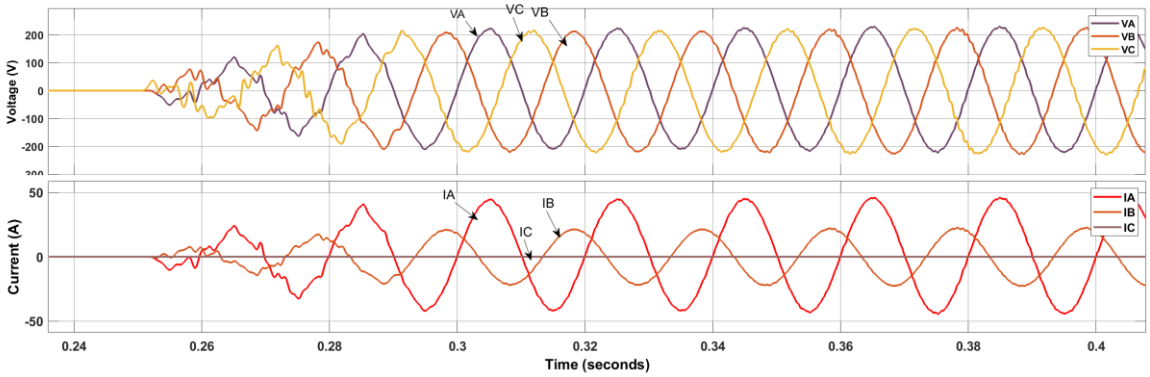

Fig. 11. Three Phase Voltage and Current for Designed Micro Grid Connected to Linear Unbalanced Resistive Loads.

6.1 Case One: Balance Resistive Linear Load

The designed microgrid is connected to a linear balanced resistive load, i.e., equal in value. Each phase is connected to 15Ω (R_a, R_b, R_c= 15Ω)), and it is implemented by the Matlab Simulink program to obtain the shape and value of each of the voltage and current feeding this type of load as shown in Fig .9. It noted through the results presented in Fig .10 at 0.25 second, the situation changes from no microgrid load to microgrid load mode with balanced resistive load. The voltages of the three phases are equal and equal to the value of the reference signal connected to the PID controller, which is within 230V (V_A=V_B=V_C =230V), and the currents I_A, I_B and I_C are equal to equal the values of the loads connected to them, which are within 18 A.

6.2 Case Two: Unbalance Resistive Linear Load

The designed microgrid is connected to a linear unbalanced resistive load, i.e., unequal in value. Each phase is connected to a load randomly selected as follows (R_a=5 Ω,R_b=10 Ω,R_c=∞), and it is implemented by the Matlab Simulink program to obtain the shape and value of each of the voltage and current feeding this type of load as shown in Fig .11. The voltages of the three phases are equal to the value of the reference signal connected to the PID controller, which is within 230V (V_A=V_B=V_C=230V). the currents I_A,$I_B$and I_C are unequal because of different values of the loads connected to them, Where I_A is recorded close to 42 A for phase A to connect it to the lowest resistance value which is 5 Ω, while for phase B it records about 20 A to connect it to a resistance value of 10Ω and phase C records zero amperes because it is open circuit as shown in Fig .11.

6.3 Case Three: Balance Inductive Linear Load

The designed microgrid is connected to a linear balanced inductive load, i.e. equal in value. Each phase is connected to a load randomly selected as follows (R_a=10 Ω and L_a=20m H,R_b=10 Ω and L_b= 20 m H, R_c=10 Ω and L_c=20m H), and it is implemented by the Matlab Simulink program to obtain the shape and value of each of the voltage and current feeding this type of load as shown in Fig .12. The voltages of the three phases are equal and equal to the value of the reference signal connected to the PID controller, which is within 230V (V_A=V_B=V_C=230V), and the currents I_A,$I_B$and I_C are equal because of equal loads connected to them, which are within 20 A as shown in Fig .12.

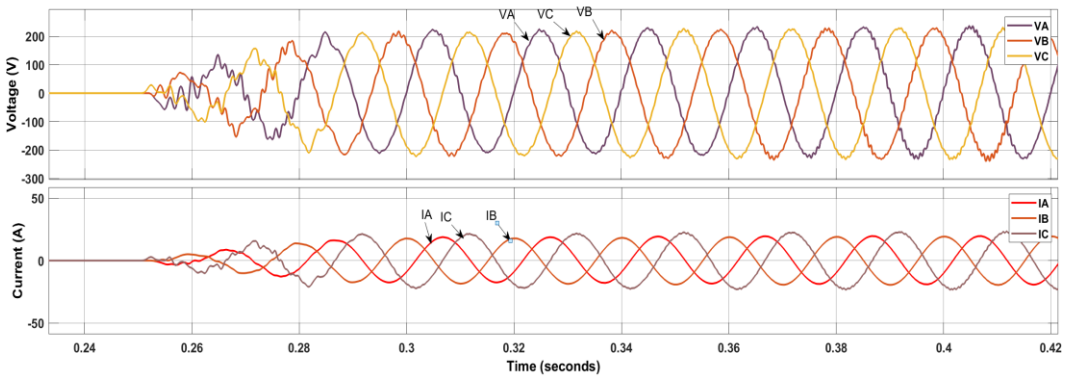

Fig. 12. Three Phase Voltage and Current for Designed Micro Grid Connected to Linear Balanced Inductive Loads.

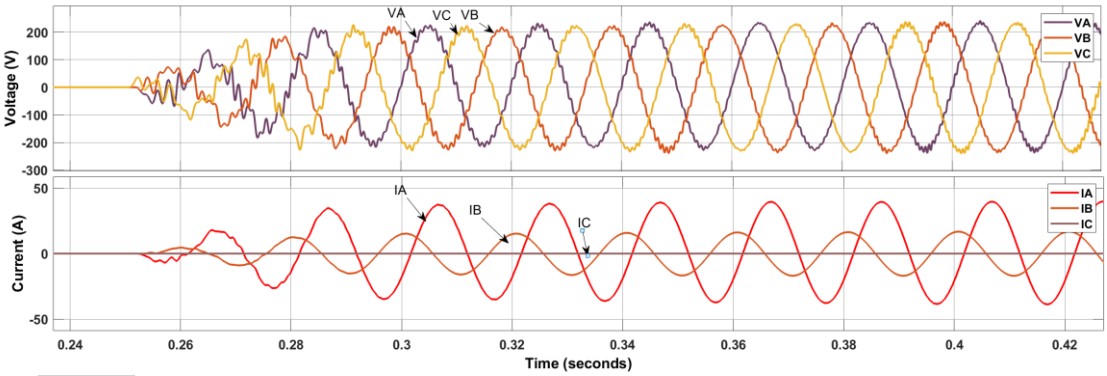

Fig. 13. Three Phase Voltage and Current for Designed Micro Grid Connected to Linear Unbalanced Inductive Loads.

6.4 Case Four: Unbalance Inductive Linear Load

The designed microgrid is connected to a linear unbalanced inductive load, i.e., unequal in value. Each phase is connected to a load randomly selected as follows (R_a=5 Ω and L_a=10m H,R_b=*10* Ω and L_b= 30 m H, R_c=∞)), and it is implemented by the Matlab Simulink program to obtain the shape and value of each of the voltage and current feeding this type of load as shown in Fig .13. The voltages of the three phases are equal and equal to the value of the reference signal connected to the PID controller, which is within 230V (V_A=V_B=V_C=230V), and the currentsI_A,$I_B$and I_C are unequal because of different values of the inductive loads connected to them, Where I_A is recorded close to 40 A for phase A to connect it to the lowest resistance and inductive value which are 5 Ω and 10m H, while for phase B it records about 19 A to connect it to a resistance value of 10Ω and inductive value of 30m H, phase C records zero amperes because it is open circuit, as shown in Fig .13**.**

6.5 Case Five: Non- Linear Load

The designed microgrid is connected to a non-linear load, i.e., unequal in value. Each phase is connected to the load as follows (R_a=20 Ω and L_a=50m H,R_{b1}=*1*Ω. R_{b2}=*60*Ω and C_b= 3000 µF, R_c=70 Ω. L_c=20m H and C_c= 5000 µF), shown in Fig .14, and it is implemented by the Matlab Simulink program to obtain the shape and value of each of the voltage and current feeding this type of load as shown in Fig .15.

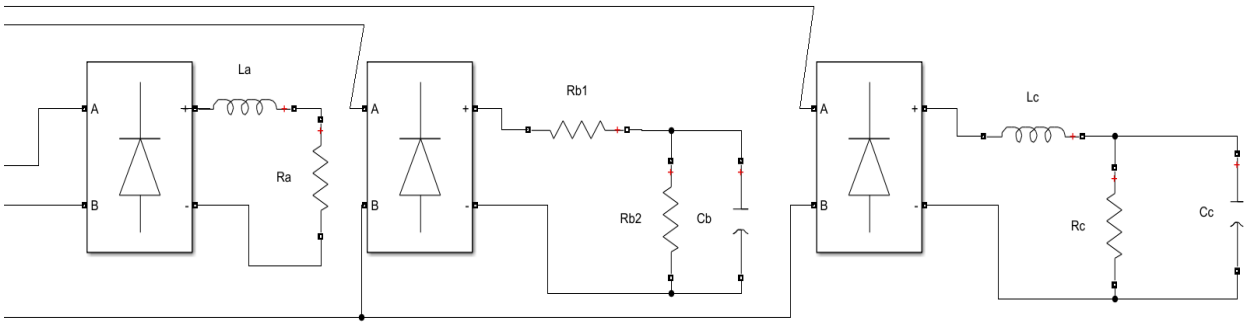

Fig. 14. Topology of Non-Linear Load Connected to Designed Micro Grid.

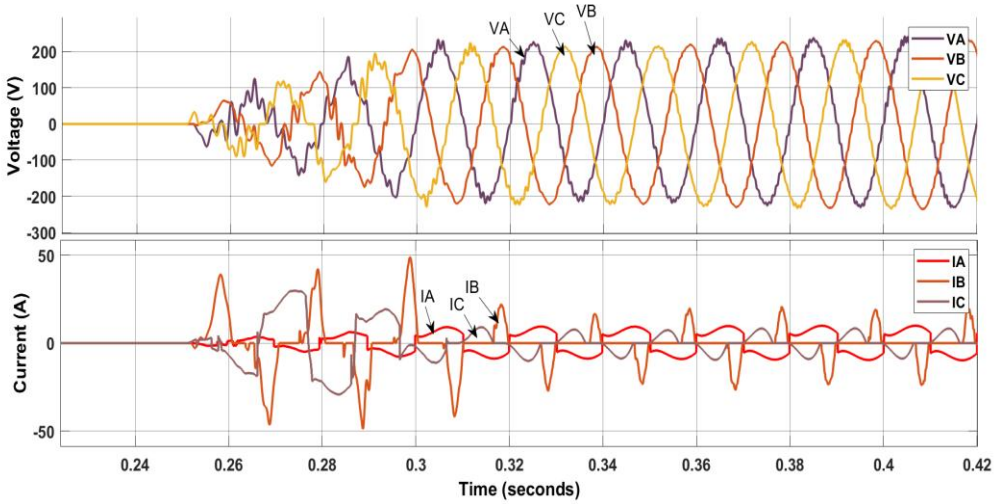

Fig. 15. Three Phase Voltage and Current for Designed Micro Grid Connected to Non-Linear Loads.

The voltages of the three phases are equal and equal to the value of the reference signal connected to the PID controller, which is within 230 v(V_A=V_B=V_C=230V), and the currentsI_A,$I_B$and I_C have not uniform shape because connected to a non-linear load, as shown in Fig .15**.** To fill the shortage of energy supplied to the consumer, the micro grid is connected to the main grid, as shown in Fig .16**.** Connecting the designed grid that relies on solar energy with another grid that relies on wind power to generate electric power and linking them together to the main grid. More details shown in Fig .16.

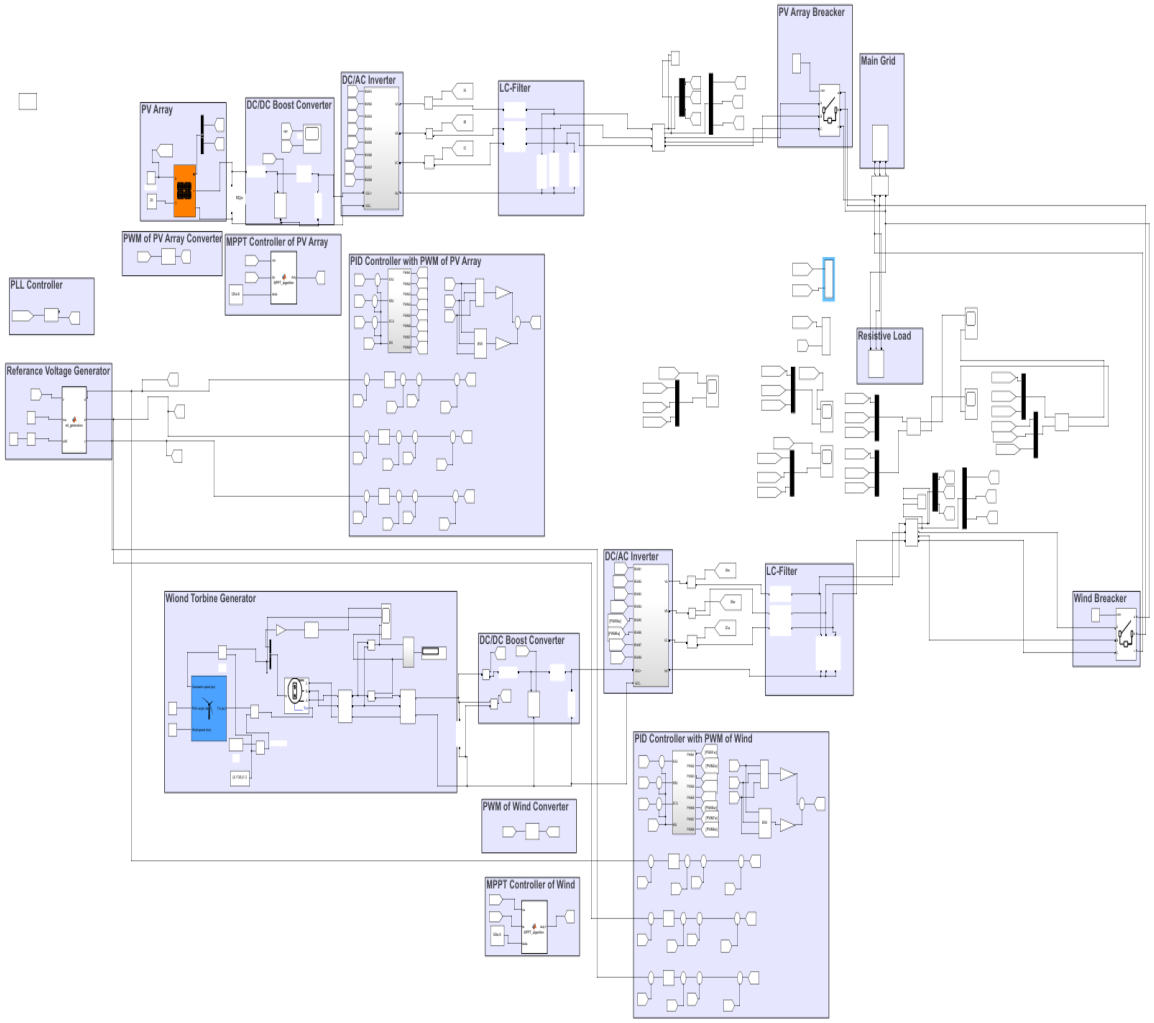

Fig. 16. Grid-Connecting Mode of Designed Micro Grid.

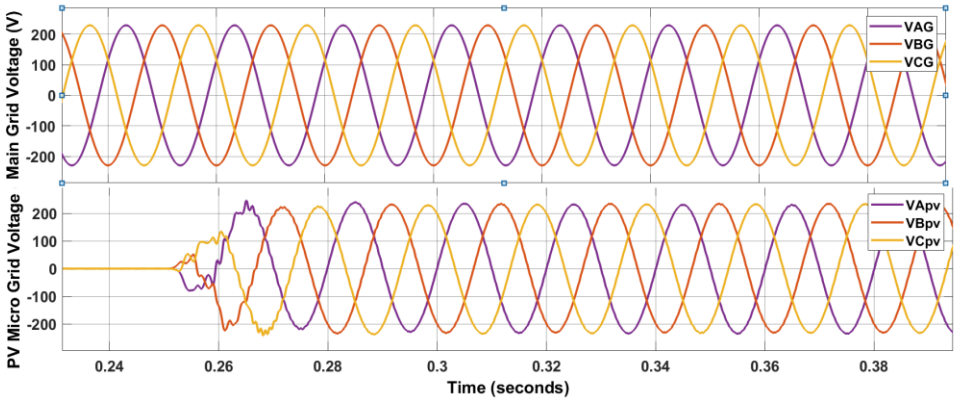

Fig. 17. The Voltage of the Main Grid is Synchronized with the Voltage of the Designed Micro Grid.

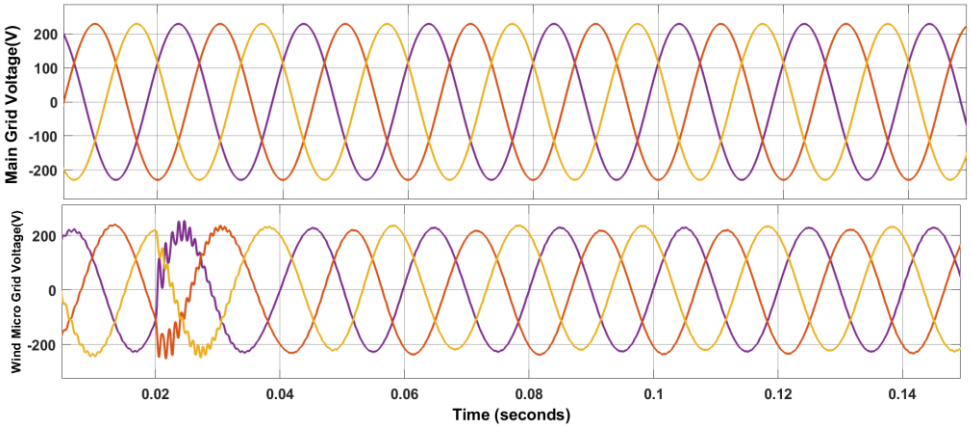

Fig. 18. The Voltage of the Main Grid is Synchronized with the Voltage of the Wind Turbin Generator Grid.

In grid-connecting mode, the PLL controller is used to match and synchronize the phases of the grids connected to the same load as shown in Fig .17, the voltage of the main grid is synchronized with the voltage generated by the designed solar power system. Fig .18 shows the frequency compatibility between the main grid and the wind energy grid. Thus the frequency control can be verified by the proposed design in Fig .18**.** The results in Fig .19 show the actual sharing between the designed grid and the network based on wind energy by supplying the active power required by the load connected to them at 0.3s and it is about 0.0364 kW because the value of the connected load is small only to implement the design and indicate the achievement of the goals for which it was designed. Fig .20 shows the lack of reactive power close to zero in both grids.

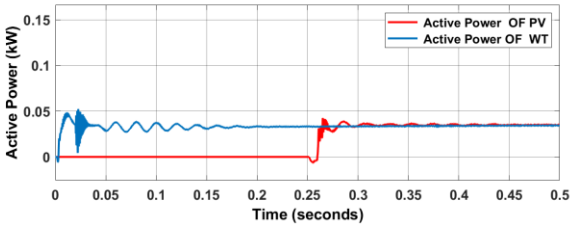

Fig. 19. Active Power Sharing between Designed Micro Grid and Wind Turbin Generator Grid.

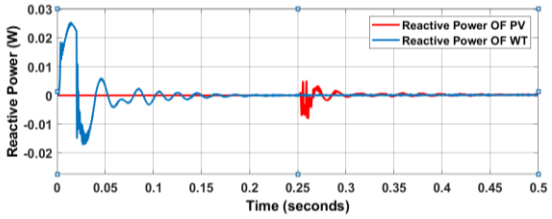

Fig. 20. Reactive Power Sharing between Designed Micro Grid and Wind Turbin Generator Grid.

7. CONCLUSION

The designed system of control of a smart grid powered by solar energy using a PV array with a proposed PID controller which selected values by PSO technique was verified, based on the results has a high control in regulating the voltage and the current supplying different types of loads linear, non-linear, balanced and unbalanced loads, after connecting the smart grid designed with the main grid to cover the shortage and working in grid connecting mode to feed the same load, condition of power-sharing was achieved for active power and reactive power due to the regulated voltage and current. Connecting the smart grid to the main via the PLL controller, the condition of regulating the frequency between both networks feeding the same load has been fulfilled.

REFERENCES

[1] Zhou X, Guo T, Ma Y. An overview on microgrid technology. 2015 IEEE international conference on mechatronics and automation (ICMA): IEEE; 2015. pp. 76-81.

[2] Bayindir R, Hossain E, Kabalci E, Perez RJIJoRER. **A comprehensive study on microgrid technology**. *International Journal of Renewable Energy Research*,2014;**4**(4):1094-1107.

[3] Asseter R, Akhil A, Marnay C, Stephens J, Dagle J, Guttromson R, Meliopoulous A, Yinger R, Eto J. **Microgrid stability definitions, analysis, and examples**. *IEEE Transactions on Power Systems*, 2019;**35**(1):13-29.

[4] Degobert P, Kreuawan S, Guillaud X. Micro-grid powered by photovoltaic and micro turbine.

[5] Lasseter R, et al. **The CERTS microgrid concept. White paper for Transmission Reliability Program, Office of Power Technologies**, *US Department of Energy*, 2002;**2**(3):30.

[6] Lee SB, Pathak C, Ramadesigan V, Gao W, Subramanian VRJJoTES. **Direct, efficient, and real-time simulation of physics-based battery models for stand-alone pv-battery microgrids**. *Journal of The Electrochemical Society*, 2017;**164**(11): E3026.

[7] Jalil MF, Khatoon S, Nasiruddin I, Bansal RJIJoM, **Simulation. Review of PV array modelling, configuration, and MPPT techniques**. *International Journal of Modelling Simulation*, 2022;**42**(4):533-550.

[8] Hasaneen B, Mohammed AAE. Design and simulation of DC/DC boost converter. 2008 12th International Middle-East Power System Conference: IEEE; 2008. pp. 335-340.

[9] Masri S, Chan P. Design and development of a DC-DC boost converter with constant output voltage. 2010 international conference on intelligent and advanced systems: IEEE; 2010. pp. 1-4.

[10] Erickson RW, Maksimovic D. Fundamentals of power electronics: Springer Science & Business Media; 2007.

[11] Kollimalla SK, Mishra MKJIToEc. **A novel adaptive P&O MPPT algorithm considering sudden changes in the irradiance**. *IEEE Transactions on Energy Conversion*,2014;**29**(3):602-610.

[12] Aboelsaud R, Ibrahim A, Garganeev AG. Voltage control of autonomous power supply systems based on PID controller under unbalanced and nonlinear load conditions. 2019 International Youth Conference on Radio Electronics, Electrical and Power Engineering (REEPE): IEEE; 2019. pp. 1-6.

[13] Luo FL, Ye H. Advanced DC/AC inverters: applications in renewable energy: CRC Press; 2017.

[14] Barr. **Pulse width modulation. Embedded Systems Programming**. *MJESP*, 2001;**14**(10):103-104.

[15] Büyük M, Tan A, Tümay M, Bayındır KÇJR, Reviews SE. **Topologies, generalized designs, passive and active damping methods of switching ripple filters for voltage source inverter: A comprehensive review**. *Renewable Sustainable Energy Reviews,* 2016;**62**:46-69.

[16] Nagrath I. Control systems engineering: New Age International; 2006.

[17] Goodwin GC, Graebe SF, Salgado ME. Control system design. Vol. 240: Prentice Hall Upper Saddle River; 2001.

[18] Wang D, Tan D, Liu LJSc. **Particle swarm optimization algorithm: an overview**. *Soft computing* ,2018;**22**(2):387-408.

[19] Solihin MI, Tack LF, Kean ML. Tuning of PID controller using particle swarm optimization (PSO). Proceeding of the international conference on advanced science, engineering and information technology; 2011. pp. 458-461.

[20] Ashenden PJ, Peterson GD, Teegarden DA. The system designer's guide to VHDL-AMS: analog, mixed-signal, and mixed-technology modeling: Elsevier; 2002.